INTERNATIONAL JOURNAL OF OPTIMIZATION IN CIVIL ENGINEERING
Int. J. Optim. Civil Eng., 2025; 15(4):543-555

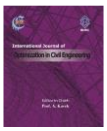

GEOMETRICAL AND MATERIAL OPTIMIZATION OF FUNCTIONALLY GRADED DOUBLY-CURVED SHELLS USING THE GREY WOLF OPTIMIZATION ALGORITHM

R. Kamgar[1*, †], F. Rahmani[2]
[1]*Department of Civil Engineering, Shahrekord University, Shahrekord, Iran*
[2]*Department of Civil Engineering, Shahid Bahonar University of Kerman, Kerman, Iran*

[DOI: 10.22068/ijoce.2025.15.4.654]

ABSTRACT

This study investigates the geometrical and material design aspects of functionally graded (FG) doubly-curved shells. The FG material system comprises a combination of metal and ceramic constituents, and the effective properties across the shell thickness are estimated using Voigt's rule of mixtures. To analyze the structural behaviour, the finite element method is employed within the framework of third-order shear and normal deformation theories. The grey wolf optimization (GWO) algorithm is implemented to achieve design optimization. The objective function aims to minimize both the maximum displacement and the fundamental dimensionless natural frequency in each optimization process individually. The findings indicate that under highly constrained boundary conditions, the curvature parameters remain constant. Conversely, for less constrained conditions, the parameter R_2 assumes a value approximately ten times greater than R_1.

Keywords: FGM, GWO algorithm, doubly-curved shell, third-order shear and normal deformation theories.

Received: 23 September 2025; Accepted: 8 November 2025

1. INTRODUCTION

Functionally Graded Materials (FGMs) represent a class of advanced composites characterized by a continuous and smooth variation in material properties throughout their volume. This gradation enhances performance by minimizing thermal conductivity, improving corrosion resistance, and reducing stress concentration, thereby mitigating typical interfacial issues such as delamination and cracking [1]. Due to these advantageous

[*]Corresponding author: Department of Civil Engineering, Shahrekord University, Shahrekord, Iran
[†]E-mail address: kamgar@sku.ac.ir (R. Kamgar)

attributes, FGMs have found widespread applications across various scientific and engineering disciplines, including mechanical, aerospace, biomedical, and defense sectors [2]. In practical contexts, computational optimization in design plays a pivotal role in maximizing the mechanical efficiency and material capabilities of structural components.

Extensive research has been conducted to examine the mechanical behaviour of doubly-curved shells. Shah and Batra [3] carried out a static analysis of laminated doubly-curved shells using the Finite Element Method (FEM) grounded in Third-Order Shear and Normal Deformation Theory (TSNDT). Choe *et al.* [4] employed the Rayleigh–Ritz method in conjunction with Higher-Order Shear Deformation Theory (HSDT) to assess such shell structures, while Han *et al.* [5] explored their vibrational responses through the Differential Quadrature Method (DQM). Moreover, Arefi *et al.* [6] analyzed the static performance of doubly-curved FG nanoshells based on a higher-order sinusoidal deformation theory, and Fazzolari *et al.* [7] examined vibration behaviour using a unified framework powered by the Generalized Differential Quadrature (GDQ) technique. Further advancements include Kwak *et al.* [8], who proposed a meshless Local Gradient Smoothing Method under First-Order Shear Deformation assumptions, and Sofiyev *et al.* [9], who studied nonlinear vibration in orthotropic FG shells.

In response to increasing demands for lightweight, resilient, and high-performance structures in modern engineering, numerous studies have focused on optimization strategies to address these challenges [10]. For instance, Salimi *et al.* [11] optimized the parameters of vibration control systems—namely tuned mass dampers and frictional tuned mass dampers—using the Multi-Objective Cuckoo Search (MOCS) algorithm. Dadkhah *et al.* [12] adopted the Water Cycle Algorithm (WCA) to refine tuned mass damper configurations under drift constraints. Kamgar *et al.* [13] applied the Grey Wolf Optimization (GWO) algorithm to design modified tuned liquid dampers considering soil-structure interactions. Etedali *et al.* [14] utilized MOCS to enhance earthquake resilience in friction isolators. The GWO algorithm has proven particularly effective for tackling complex engineering design tasks [15].

Optimization of composite structures has also garnered significant attention [16]. For example, Lieu *et al.* [17] applied isogeometric analysis combined with an adaptive hybrid firefly algorithm for optimizing the shape and size of FG sandwich plates. Wang *et al.* [18] investigated bi-directional FG plate optimization using MOPSO and Generalized Isogeometric Analysis (GIGA). Yuan *et al.* [19] examined initial failure loads in doubly-curved sandwich shells through a honeybee-inspired algorithm alongside TSNDT-based FEM. Ghasemi *et al.* [20] employed a regenerated Genetic Algorithm (GA) to determine optimal buckling loads in polymer composite shells. Imran *et al.* [21] explored optimal design strategies for submerged cylindrical pressure hulls under hydrostatic load via analytical and MOGA methods, targeting improved buckling capacity and minimized buoyancy. Kaveh *et al.* [22] proposed two new multi-objective optimization algorithms with high-quality solutions in engineering problems. Kaveh *et al.* [23] resolved the weakness points of conventional gradient-based optimization techniques (i.e., getting trapped in local optimal solutions and being highly sensitive to initial conditions) by presenting a hybrid approach grounded in rigorous mathematical foundations, established principles of structural mechanics, and effective stochastic search strategies.

Additional work by Rahmani *et al.* [24] utilized MOPSO to derive optimal material

[DOI: 10.22068/ijoce.2025.15.4.654]

distributions in porous FG plates, combining Isogeometric Analysis (IGA) with Carrera Unified Formulation (CUF) for mechanical evaluation. Wang *et al.* [25] proposed a multi-objective isogeometric optimization framework aimed at maximizing first-order natural frequency and minimizing static shape error in piezoelectric FG plates.

The present study focuses on the optimal design of doubly-curved FG shells. Initially, the kinematic relations are established using TSNDT, and the equations of motion are derived via Hamilton's principle. The FEM is implemented to assess both static and dynamic responses across various FGM shell configurations. A single-objective GWO algorithm is employed to perform optimization targeting either the minimization of displacement or the maximization of the first natural frequency. Multiple numerical case studies are presented to evaluate the impact of boundary conditions, power-law index, curvature ratio, and geometric proportions, with results validated against existing literature benchmarks.

2. MATHEMATICAL FORMULATION

2.1. FGMs

Consider a doubly-curved shell composed of a unidirectional functionally graded (FG) material, with a thickness denoted by *h*, as illustrated in Figure 1. The variation of the elastic properties through the thickness direction of the FG material is characterized by the rule of mixtures approach, as described in [26, 27].

$$\begin{aligned} E(\zeta) &= E_{bot} + (E_{top} - E_{bot}) \times V_c \\ \rho(\zeta) &= \rho_{bot} + (\rho_{top} - \rho_{bot}) \times V_c \\ \nu(\zeta) &= \nu_{bot} + (\nu_{top} - \nu_{bot}) \times V_c \end{aligned} \tag{1}$$

The subscripts "bot" and "top" denote the bottom and top surfaces of the doubly-curved functionally graded (FG) shell, respectively. The ceramic volume fraction (CVF), denoted by V_c, can be expressed in the form of a power-law function as follows:

$$V_c = \left(\frac{1}{2} + \frac{\zeta}{h}\right)^n \tag{2}$$

The parameters *h* and *n* denote the total thickness of the shell and the power-law index, respectively, where the latter governs the variation of the thickness profile of the functionally graded (FG) material.

[DOI: 10.22068/ijoce.2025.15.4.654]

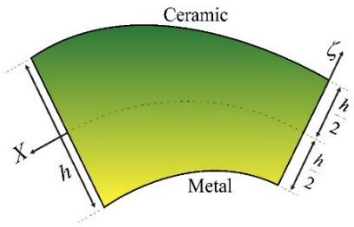

Figure 1: Variation of the elastic properties of the functionally graded (FG) doubly-curved shell along the thickness direction [28].

2.2. THE TSNDT FOR A DOUBLY-CURVED FG SHELL

In the present study, a third-order shear deformation theory (TSNDT) is employed to investigate the bending and free vibration behaviour of functionally graded (FG) spherical shells. The fundamental geometry and coordinate system of the doubly-curved FG shell are illustrated in Figure 2. The x and y axes lie along the in-plane directions, whereas the ζ coordinate is oriented normal to the shell's mid-surface. The parameters R_1 and R_2 represent the radii of curvature of the shell's mid-surface in the x and y directions, respectively.

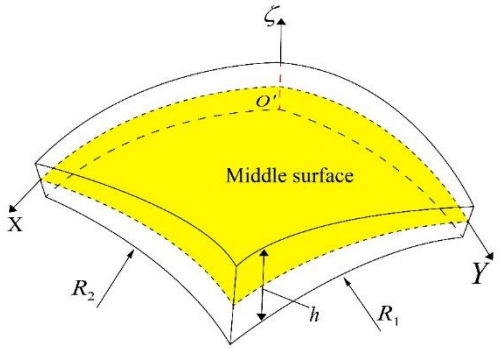

Figure 2: Fundamental geometry of the functionally graded (FG) doubly-curved shell [28].

In the framework of third-order shear deformation theory (TSNDT), the displacement field variables u_i are approximated using a complete cubic distribution along the thickness direction, denoted by ζ, as formulated by [3].

$$u_i(x,y,\zeta,t) = \sum_{j=0}^{3} \zeta^j u_{ij}(x,y,t) \qquad i = 1,\ 2,\ 3 \tag{3}$$

In this formulation, the in-plane displacements are represented by the components u_1 and u_2, while the transverse displacement of a point located on the mid-surface of the shell is

[DOI: 10.22068/ijoce.2025.15.4.654]

denoted by the component u_3. Assuming small linear deformations, the corresponding strain components can be expressed as follows:

$$\begin{aligned}
\varepsilon_{11} &= \frac{1}{H_1}\left(u_{1,x} + \frac{u_3}{R_1}\right) \\
\varepsilon_{22} &= \frac{1}{H_1}\left(u_{2,y} + \frac{u_3}{R_2}\right) \\
\varepsilon_{33} &= \frac{1}{H_1}\left(u_{3,\zeta}\right) \\
\gamma_{12} &= \frac{1}{H_1}u_{2,x} + \frac{1}{H_2}u_{1,y} \\
\gamma_{13} &= \frac{1}{H_1}\left(u_{3,x} - \frac{u_1}{R_1}\right) + u_{1,\zeta} \\
\gamma_{23} &= \frac{1}{H_2}\left(u_{3,y} - \frac{u_2}{R_2}\right) + u_{2,\zeta} \\
H_1 &= 1 + \frac{\zeta}{R_1} \\
H_2 &= 1 + \frac{\zeta}{R_2}
\end{aligned} \tag{4}$$

The strain vector can be decomposed into two components: the in-plane strain components ε_p and the normal strain component ε_n, as expressed below:

$$\varepsilon_p = [\varepsilon_{11}, \varepsilon_{22}, \gamma_{12}]^T \qquad \varepsilon_n = [\gamma_{23}, \gamma_{13}, \varepsilon_{33}]^T \tag{5}$$

By substituting Eq. (3) into Eq. (4), the strain matrix is derived as follows:

$$\varepsilon = Z_i(\zeta)\ O\ d_i \qquad i = 0,\ 1,\ 2,\ 3 \tag{6}$$

where O, Z_i, and d_i represent the differential operator matrix and the Z matrix, as defined in Eq. (7).

[DOI: 10.22068/ijoce.2025.15.4.654]

$$O^T=\begin{bmatrix} \frac{\partial}{\partial x} & 0 & \frac{\partial}{\partial y} & 0 & 0 & 0 & 1 & 0 & 0 \\ 0 & \frac{\partial}{\partial y} & 0 & \frac{\partial}{\partial x} & 0 & 1 & 0 & 0 & 0 \\ 0 & 0 & 0 & 0 & 1 & 0 & 0 & \frac{\partial}{\partial y} & \frac{\partial}{\partial x} \end{bmatrix}$$

$$Z_i=\begin{bmatrix} \frac{\zeta^i}{H_1} & 0 & 0 & 0 & \frac{\zeta^i}{R_1H_1} & 0 & 0 & 0 & 0 \\ 0 & \frac{\zeta^i}{H_2} & 0 & 0 & \frac{\zeta^i}{R_2H_2} & 0 & 0 & 0 & 0 \\ 0 & 0 & 0 & 0 & i\zeta^{i-1} & 0 & 0 & 0 & 0 \\ 0 & 0 & 0 & 0 & 0 & \alpha_2 & 0 & \frac{\zeta^i}{H_2} & 0 \\ 0 & 0 & 0 & 0 & 0 & 0 & \alpha_1 & 0 & \frac{\zeta^i}{H_1} \\ 0 & 0 & \frac{\zeta^i}{H_2} & \frac{\zeta^i}{H_1} & 0 & 0 & 0 & 0 & 0 \end{bmatrix} \tag{7}$$

$$\alpha_1=\frac{i\zeta^{i-1}+(i-1)\zeta^i/R_1}{H_1}$$

$$\alpha_2=\frac{i\zeta^{i-1}+(i-1)\zeta^i/R_2}{H_2}$$

The displacement vector is expressed as follows:

$$d_i=[u_{1i},u_{2i},u_{3i}]^T \qquad i=0,\ 1,\ 2,\ 3 \tag{8}$$

The stress–strain relationships for the functionally graded (FG) shell are formulated based on Hooke's law, assuming the material behaves in a linear elastic manner.

$$\sigma_{ij}=C_{ijkl}\varepsilon_{kl} \qquad i,j,k,l=1,\ 2,\ 3 \tag{9}$$

[DOI: 10.22068/ijoce.2025.15.4.654]

where C_{ijkl} denotes the fourth-order elasticity tensor, which, for functionally graded materials (FGMs), can be expressed as:

$$\begin{Bmatrix}\sigma_{11}\\ \sigma_{22}\\ \sigma_{33}\\ \tau_{23}\\ \tau_{13}\\ \tau_{12}\end{Bmatrix}=\begin{bmatrix}C_{11}^{\zeta} & C_{12}^{\zeta} & C_{13}^{\zeta} & 0 & 0 & 0\\ C_{12}^{\zeta} & C_{22}^{\zeta} & C_{23}^{\zeta} & 0 & 0 & 0\\ C_{13}^{\zeta} & C_{23}^{\zeta} & C_{33}^{\zeta} & 0 & 0 & 0\\ 0 & 0 & 0 & C_{44}^{\zeta} & 0 & 0\\ 0 & 0 & 0 & 0 & C_{55}^{\zeta} & 0\\ 0 & 0 & 0 & 0 & 0 & C_{66}^{\zeta}\end{bmatrix}\begin{Bmatrix}\varepsilon_{11}\\ \varepsilon_{22}\\ \varepsilon_{33}\\ \gamma_{23}\\ \gamma_{13}\\ \gamma_{12}\end{Bmatrix} \tag{10}$$

$$C_{11}^{\zeta}=C_{22}^{\zeta}=C_{33}^{\zeta}=\frac{(1-\nu(\zeta))E(\zeta)}{(1+\nu(\zeta))(1-2\nu(\zeta))}$$

$$C_{12}^{\zeta}=C_{13}^{\zeta}=C_{23}^{\zeta}=\frac{\nu(\zeta)E(\zeta)}{(1+\nu(\zeta))(1-2\nu(\zeta))}$$

$$C_{44}^{\zeta}=C_{55}^{\zeta}=C_{66}^{\zeta}=\frac{E(\zeta)}{2(1+\nu(\zeta))}$$

Similarly, the stress vector comprises six components, which are classified into in-plane and out-of-plane (normal) stresses as follows:

$$\sigma_p=[\sigma_{11},\sigma_{22},\tau_{12}]^T \qquad \sigma_n=[\tau_{23},\tau_{13},\sigma_{33}]^T \tag{11}$$

Hamilton's principle is employed to derive the governing equation of motion and the corresponding boundary conditions for the functionally graded (FG) shell. Here, ρ represents the mass density, q denotes the external work, and the $\dot{d}$ terms indicate velocity components in the x, y, and ζ directions, respectively. The stiffness (K_{ij}^{e}) and mass matrix (M^{e}) of each element can be computed as follows. Also, the work done by external work (F^{e}) can be derived as follows:

$$K_{ij}^{e}=\sum_{i=1}^{ng}\sum_{j=1}^{ng}B^{T}(\xi_i,\eta_i)DB(\xi_j,\eta_j)\;w_i w_j\left|J\right|$$

$$D_{ij}=\sum_{k=1}^{N}\int_{\zeta_k}^{\zeta_{k+1}}Z_i^{T}C^{\zeta}Z_j\;d\zeta$$

$$M^{e}=\int_{\zeta}\int_{S}\rho(\zeta)\left\{\frac{\delta\dot{u}_1}{\partial t}\frac{\dot{u}_1}{\partial t}+\frac{\delta\dot{u}_2}{\partial t}\frac{\dot{u}_2}{\partial t}+\frac{\delta\dot{u}_3}{\partial t}\frac{\dot{u}_3}{\partial t}\right\}\;dS)\;H_1H_2\;d\zeta \tag{12}$$

$$F^{e}=\int_{S}\delta d_i^{T}(\zeta)^{i}\mathrm{q}\;dA \qquad i=0,\;1,\;2,\;3$$

[DOI: 10.22068/ijoce.2025.15.4.654]

3. OPTIMIZATION METHODOLOGY

3.1. Grey wolf optimization algorithm

The GWO algorithm studied here is a single-objective optimization algorithm inspired by the natural process of four gray wolves hunting based on three main hunting steps (i.e., search, siege, and attack) [29]. In fact, the social hierarchy of wolves is considered here to design the GWO algorithm. In this algorithm, the first, second, and third solutions are named as α, β, and δ, respectively, while the other candidates are considered as ω [29]. The three above-mentioned wolves (i.e., α, β, and δ) are followed by the wolves $\bar{Y}$ as the following equation [29]:

$$\begin{aligned} D &= \left| C.\bar{Y}_p(l) - \bar{Y}(l) \right| \\ \bar{Y}(l+1) &= \bar{Y}_p(l) - A.D \end{aligned} \tag{13}$$

In Eq. (13), A and C show the coefficient vectors that can be calculated. Also, the parameter $\bar{Y}_p(l)$ represents the position of the wounded [29].

$$A = 2ar_1 - a, \quad C = 2r_2 \tag{14}$$

where a shows a scalar parameter that reduces from two to zero during the repetition, also, two random vectors (i.e., $\boldsymbol{r}_1$ and $\boldsymbol{r}_2$) are considered to be between zero and one. Finally, in the GWO, the three best solutions are stored in the optimization process. In contrast, the other wolves are forced to update their positions based on the best solutions. The following equations are used to achieve this aim. Therefore, a random position in a circle defined by α, β, and δ approximates the final position [29].

$$\begin{aligned} D_\alpha &= \left| C_1\bar{Y}_\alpha - \bar{Y} \right| \\ D_\beta &= \left| C_2\bar{Y}_\beta - \bar{Y} \right| \\ D_\delta &= \left| C_3\bar{Y}_\delta - \bar{Y} \right| \\ \bar{Y}_1 &= \bar{Y}_\alpha - A_1.D_\alpha \\ \bar{Y}_2 &= \bar{Y}_\beta - A_2.D_\beta \\ \bar{Y}_3 &= \bar{Y}_\delta - A_3.D_\delta \\ \bar{Y}(l+1) &= \frac{\bar{Y}_1(l) + \bar{Y}_2(l) + \bar{Y}_3(l)}{3} \end{aligned} \tag{15}$$

The detailed information for implementation in the optimization problem can be found in Ref. [29].

[DOI: 10.22068/ijoce.2025.15.4.654]

4. RESULTS AND DISCUSSION

4.1. Optimization problems

In this subsection, the results of the optimization problems are presented. It is noteworthy that all computations were performed on a system equipped with an Intel(R) Xeon(R) E5-2680 2.40 GHz processor and 128 GB of RAM. The formulation of the optimization problem, including the upper and lower bounds and the various constraint scenarios considered, is defined as follows:

$$\begin{aligned} &\text{Find:} && R_1,\ R_2 \text{ and } n \\ &\text{minimize:} && \begin{cases} \text{max normalized displacement (O.F 1)} \\ \dfrac{1}{\bar{\omega}_1} \text{ (O.F 2)} \end{cases} \\ &\text{Subjected to:} && \begin{cases} 1.0 \le \dfrac{R_1}{a} \le 200 \\ 1.0 \le \dfrac{R_2}{R_1} \le 10 \\ 0.0 \le n \le \infty \end{cases} \end{aligned} \tag{16}$$

According to Eq. (16), the optimization process aims to identify the optimal parameters for the geometry of shell structures, specifically, R_1 and R_2, which represent the curvature of the shell's middle surface in the x- and y-directions, respectively, as well as the material configuration across the shell thickness, denoted by n. The objective functions in this process involve minimizing the normalized displacement and maximizing the first dimensionless frequency of the functionally graded (FG) shell.

It is assumed that the shell consists of a composite material made from stainless steel (SUS304) and alumina (Al_2O_3). The corresponding material properties are presented in Table 1. Tables (2-4) summarize the results obtained from the optimization process using various methods considered.

Table 1: Isotropic mechanical properties of the FGMs

Properties		E (GPa)	ν	ρ (kg/m^3)
Material [30]	SUS304	201.04	0.3262	8166
	Al_2O_3	349.55	0.24	3800

For all scenarios (i.e., boundary conditions, *a/h* ratios, and objective functions), the power index values are equal to zero, which means that fully ceramic material (i.e., a material with more stiffness and low density) shells have been used throughout the thickness direction. The curvature values (i.e., R_1 and R_2) are constant when the boundary conditions are more constrained. In contrast, the values of R_2 are ten times R_1 for less restricted boundary conditions (i.e., SFSF, SFSS, SFSC, and CFCF).

[DOI: 10.22068/ijoce.2025.15.4.654]

Table 2: The obtained results for the GWO problem for *a/h*=100

B.C.	O.F 1				O.F 2			
	$R_1(m)$	$R_2(m)$	n	V.O.F	$R_1(m)$	$R_2(m)$	n	V.O.F
CCCC	1	1	0	0.0005	1	1	0	104.7109
SCSC	1	1	0	0.0009	1	1	0	101.5538
SSSC	1	1	0	0.0011	1	1	0	98.0776
SSSS	1	1	0	0.0011	1	1	0	96.2968
CFCF	1	10	0	0.0023	1	1	0	37.4748
SFSC	1	9.9932	0	0.0350	1	2.1832	0	14.2269
SFSS	1.014	1.014	0	0.9962	2.1605	2.1605	0	4.5897
SFSF	1.0166	1.0166	0	1.0976	1.6504	1.6504	0	4.0163

Table 3: The obtained results for the GWO problem for *a/h*=20

B.C.	O.F 1				O.F 2			
	$R_1(m)$	$R_2(m)$	n	V.O.F	$R_1(m)$	$R_2(m)$	n	V.O.F
CCCC	1	1	0	0.0165	1	1	0	27.9765
SCSC	1	1	0	0.0237	1	1	0	23.0304
SSSC	1	1	0	0.0290	1	1	0	20.8934
SSSS	1	1	0	0.0314	1	1	0	19.9035
CFCF	1	10	0	0.0451	1	1	0	17.8105
SFSC	1	10	0	0.6104	1	10	0	5.2731
SFSS	1.181	1.181	0	1.2440	1.5777	1.5777	0	3.9379
SFSF	1.0517	1.0517	0	1.4021	1.2590	1.2590	0	3.3959

Table 4: The obtained results for the GWO problem for *a/h*=10

B.C.	O.F 1				O.F 2			
	$R_1(m)$	$R_2(m)$	n	V.O.F	$R_1(m)$	$R_2(m)$	n	V.O.F
CCCC	1	1	0	0.0573	1	1	0	16.3948
SCSC	1	1	0	0.0850	1	1	0	13.1659
SSSC	1	1	0	0.1075	1	1	0	11.6882
SSSS	1	1	0	0.1243	1	1	0	10.8538
CFCF	1	10	0	0.1347	1	1	0	10.5812
SFSC	1	10	0	1.1647	1	10	0	3.8476
SFSS	200	2000	0	1.4489	1.6666	1.6666	0	3.5460
SFSF	200	2000	0	1.6852	1.2453	1.2453	0	2.9658

[DOI: 10.22068/ijoce.2025.15.4.654]

5. CONCLUSION

This paper explores the material and geometric optimization of functionally graded (FG) doubly-curved shell structures. A mathematical model based on the Third-Order Shear and Normal Deformation Theory (TSNDT) is developed to analyze the bending and vibrational behaviour of these structures. The finite element method (FEM) is employed to compute deflections and natural frequencies. Voigt's rule of mixtures is applied to characterize the through-thickness behaviour of FG materials. A single-objective Grey Wolf Optimizer (GWO) is used to optimize both the curvature and material distribution in FG shells, targeting two distinct objectives: (i) minimization of maximum central deflection and (ii) maximization of the first natural frequency. The study incorporates both normal and shear deformation effects without using shear correction factors. The results show that an increase in the curvature ratio (R_2/R_1) leads to a rise in deflection and a reduction in the fundamental natural frequency. Also, under GWO optimization, varying boundary conditions and *a/h* ratio result in different curvature profiles, although the power-law index remains unchanged across objective functions. In addition, with more constrained boundary conditions, the curvature parameters R_1 and R_2 remain constant. Conversely, for less constrained setups (e.g., SFSF, SFSS, SFSC, and CFCF), R_2 is approximately ten times greater than R_1.

6. ACKNOWLEDGMENTS

The authors would like to show their appreciation to the HPC center (Shahr-e-Kord University, Iran) for their collaboration in offering computational clusters, which was a great help in completing this work.

REFERENCE

1. Li Y, Feng Z, Hao L, Huang L, Xin C, Wang Y, Bilotti E, Essa K, Zhang H, Li Z, Yan F, Peijs T. A review on functionally graded materials and structures via additive manufacturing: from multi-scale design to versatile functional properties. *Adv Mater Technol*. 2020;**5**(6):1900981.
2. Saleh B, Jiang J, Fathi R, Al-hababi T, Xu Q, Wang L, Song D, Ma A. 30 Years of functionally graded materials: an overview of manufacturing methods, applications and future challenges. *Compos Part B Eng*. 2020;**201**:108376.
3. Shah PH, Batra RC. Stretching and bending deformations due to normal and shear tractions of doubly curved shells using third-order shear and normal deformable theory. *Mech Adv Mater Struct*. 2018;**25**(15-1):1276–96.
4. Choe K, Kim K, Wang Q. Dynamic analysis of composite laminated doubly-curved revolution shell based on higher order shear deformation theory. *Compos Struct*. 2019;**225**:111155.
5. Han P, Ri K, Choe K, Han Y. Vibration analysis of rotating cross-ply laminated cylindrical, conical and spherical shells by using weak-form differential quadrature method. *J Braz Soc Mech Sci Eng*. 2020;**42**(7):352.

[DOI: 10.22068/ijoce.2025.15.4.654]

6. Arefi M, Mohammad-Rezaei Bidgoli E, Civalek O. Bending response of FG composite doubly curved nanoshells with thickness stretching via higher-order sinusoidal shear theory. *Mech Based Des Struct Mach*. 2020:1–29.
7. Fazzolari FA, Viscoti M, Dimitri R, Tornabene F. 1D-Hierarchical Ritz and 2D-GDQ formulations for the free vibration analysis of circular/elliptical cylindrical shells and beam structures. *Compos Struct*. 2021;**258**:113338.
8. Kwak S, Kim K, Ri Y, Jong G, Ri H. Natural frequency calculation of open laminated conical and cylindrical shells by a meshless method. *Eur Phys J Plus*. 2020;**135**(5):434.
9. Sofiyev AH, Turan F, Zerin Z. Large-amplitude vibration of functionally graded orthotropic double-curved shallow spherical and hyperbolic paraboloidal shells. *Int J Press Vessels Pip*. 2020;**188**:104235.
10. Kisi O, Mansouri I, Awoyera PO, Lee CH. Modeling flexural overstrength factor for steel beams using heuristic soft-computing methods. *Structures*. 2021;**34**:3238–46.
11. Salimi M, Kamgar R, Heidarzadeh H. An evaluation of the advantages of friction TMD over conventional TMD. *Innov Infrastruct Solut*. 2021;**6**(2):95.
12. Dadkhah M, Kamgar R, Heidarzadeh H, Jakubczyk-Gałczyńska A, Jankowski R. Improvement of performance level of steel moment-resisting frames using tuned mass damper system. *Appl Sci*. 2020;**10**(10):3403.
13. Kamgar R, Gholami F, Zarif Sanayei HR, Heidarzadeh H. Modified tuned liquid dampers for seismic protection of buildings considering soil–structure interaction effects. *Iran J Sci Technol Trans Civ Eng*. 2020;**44**(1):339–54.
14. Etedali S, Hasankhoie K, Sohrabi MR. Optimal design of pure-friction isolators with and without restoring device: a multi-objective cuckoo search-based approach for seismic-excited structures. *Structures*. 2020;**25**:708–19.
15. Mirjalili S. How effective is the grey wolf optimizer in training multi-layer perceptrons. *Appl Intell*. 2015;**43**(1):150–61.
16. Kaveh A, Bakhshpoori T. *Cuckoo Search Algorithm*. Springer; 2019.
17. Lieu QX, Lee J, Lee D, Lee S, Kim D, Lee J. Shape and size optimization of functionally graded sandwich plates using isogeometric analysis and adaptive hybrid evolutionary firefly algorithm. *Thin-Walled Struct*. 2018;**124**:588–604.
18. Wang C, Koh JM, Yu T, Xie NG, Cheong KH. Material and shape optimization of bi-directional functionally graded plates by GIGA and an improved multi-objective particle swarm optimization algorithm. *Comput Methods Appl Mech Eng*. 2020;**366**:113017.
19. Yuan L, Taetragool U, Batra RC. Optimum first failure loads of one- and two-core doubly curved sandwich shells. *AIAA J*. 2020;**58**(8):3665–79.
20. Ghasemi AR, Tabatabaeian A, Hajmohammad MH, Tornabene F. Multi-step buckling optimization analysis of stiffened and unstiffened polymer matrix composite shells: a new experimentally validated method. *Compos Struct*. 2021;**273**:114280.
21. Imran M, Shi D, Tong L, Elahi A, Waqas HM, Uddin M. Multi-objective design optimization of composite submerged cylindrical pressure hull for minimum buoyancy factor and maximum buckling load capacity. *Defence Technol*. 2021;**17**(4):1190–206.
22. Kaveh A, Shirzadi Javid AA, Vazirinia Y. Multi-objective variants of water strider algorithm for construction engineering optimization problems. *Period Polytech Civ Eng*. 2025.

[DOI: 10.22068/ijoce.2025.15.4.654]

23. Kaveh A, Raissi Dehkordi M, Shaghaghian AH. A neuro-gradient evolution method for simultaneous size and layout optimization of truss structures in the combined domain of variables. *Structures*. 2025;**79**:109469.
24. Rahmani F, Kamgar R, Rahgozar R. Optimum material distribution of porous functionally graded plates using Carrera unified formulation based on isogeometric analysis. *Mech Adv Mater Struct*. 2021:1–15.
25. Wang C, Yu T, Shao G, Bui TQ. Multi-objective isogeometric integrated optimization for shape control of piezoelectric functionally graded plates. *Comput Methods Appl Mech Eng*. 2021;**377**:113698.
26. Elishakoff IA, Demetris A, Gentilini C. *Mechanics of Functionally Graded Material Structures*. World Scientific; 2015.
27. Rahmani F, Kamgar R, Rahgozar R. Finite element analysis of functionally graded beams using different beam theories. *Civil Eng J*. 2020;**6**(11):2086–102.
28. Kamgar R, Rahmani F, Rahgozar R. Geometrical and material optimization of the functionally graded doubly-curved shell by metaheuristic optimization algorithms. *Structures*. 2024;**62**:106254.
29. Mirjalili S, Mirjalili SM, Lewis A. Grey wolf optimizer. *Adv Eng Softw*. 2014;**69**:46–61.
30. Zare Jouneghani F, Dimitri R, Bacciocchi M, Tornabene F. Free vibration analysis of functionally graded porous doubly-curved shells based on the first-order shear deformation theory. *Appl Sci*. 2017;**7**(12):1252.

[DOI: 10.22068/ijoce.2025.15.4.654]